Diffusion MRI Metrics Characterize Postoperative Clinical Outcomes After Surgery for Cervical Spondylotic Myelopathy

Justin K. Zhang, MD, MSCI *§, **Saad Javeed, MD, MSCI***, **Jacob K. Greenberg, MD, MSCI***, **Salim Yakdan, MD, MSCI***, **Muhammad I. Kaleem, MBBS***, **Kathleen S. Botterbush, BS***, **Braeden Benedict, MS***, **Christopher F. Dibble, MD, PhD***, **Peng Sun, PhD**‡, **Brandon Sherrod, MD**§, **Andrew T. Dailey, MD**§, **Erica F. Bisson, MD, MPH**§, **Mark Mahan, MD**§, **Marcus Mazur, MD**§, **Sheng-Kwei Song, PhD***, **Wilson Z. Ray, MD, MBA***

*Department of Neurological Surgery, Washington University School of Medicine, Saint Louis, Missouri, USA; ‡Department of Imaging Physics, UT MD Anderson Cancer Center, Houston, Texas, USA; §Department of Neurological Surgery, University of Utah, Salt Lake City, Utah, USA

Correspondence: Wilson Z. Ray, MD, Department of Neurological Surgery, Washington University School of Medicine, 660 S. Euclid Ave, Campus Box 8057, St. Louis, MO 63110, USA. Email: rayz@wustl.edu

Received, September 16, 2023; **Accepted,** April 16, 2024; **Published Online,** June 21, 2024.

Neurosurgery 96:69–77, 2025 https://doi.org/10.1227/neu.0000000000003037

BACKGROUND AND OBJECTIVES: Advanced diffusion-weighted MRI (DWI) modeling, such as diffusion tensor imaging (DTI) and diffusion basis spectrum imaging (DBSI), may help guide rehabilitation strategies after surgical decompression for cervical spondylotic myelopathy (CSM). Currently, however, postoperative DWI is difficult to interpret, owing to signal distortions from spinal instrumentation. Therefore, we examined the relationship between postoperative DTI/DBSI—extracted from the rostral C3 spinal level—and clinical outcome measures at 2-year follow-up after decompressive surgery for CSM.

METHODS: Fifty patients with CSM underwent complete clinical and DWI evaluation—followed by DTI/DBSI analysis—at baseline and 2-year follow-up. Clinical outcomes included the modified Japanese Orthopedic Association score and comprehensive patient-reported outcomes. DTI metrics included apparent diffusion coefficient, fractional anisotropy, axial diffusivity, and radial diffusivity. DBSI metrics evaluated white matter tracts through fractional anisotropy, fiber fraction, axial diffusivity, and radial diffusivity as well as extra-axonal pathology through restricted and nonrestricted fraction. Cross-sectional Spearman's correlations were used to compare postoperative DTI/DBSI metrics with clinical outcomes.

RESULTS: Twenty-seven patients with CSM, including 15, 7, and 5 with mild, moderate, and severe disease, respectively, possessed complete baseline and postoperative DWI scans. At 2-year follow-up, there were 10 significant correlations among postoperative DBSI metrics and postoperative clinical outcomes compared with 3 among postoperative DTI metrics. Of the 13 significant correlations, 7 involved the neck disability index (NDI). The strongest relationships were between DBSI axial diffusivity and NDI ($r = 0.60$, $P < .001$), DBSI fiber fraction and NDI ($r_s = -0.58$, $P < .001$), and DBSI restricted fraction and NDI ($r_s = 0.56$, $P < .001$). The weakest correlation was between DTI apparent diffusion coefficient and NDI ($r = 0.35$, $P = .02$).

CONCLUSION: Quantitative measures of spinal cord microstructure after surgery correlate with postoperative neurofunctional status, quality of life, and pain/disability at 2 years after decompressive surgery for CSM. In particular, DBSI metrics may serve as meaningful biomarkers for postoperative disease severity for patients with CSM.

KEY WORDS: Cervical spondylotic myelopathy, Diffusion-weighted imaging, Magnetic resonance imaging, Postoperative MRI

ABBREVIATIONS: ADC, apparent diffusion coefficient; **CSM,** cervical spondylotic myelopathy; **DASH,** disability of the arm, shoulder, and hand; **DBSI,** diffusion basis spectrum imaging; **FA,** fractional anisotropy; **MCID,** minimal clinically important difference; **MDI,** myelopathy disability index; **mJOA,** modified Japanese Orthopedic Association score; **NDI,** neck disability index; **PROM,** patient-reported outcome; **SF-36 MCS,** 36-item short-form survey mental component summary; **SF-36 PCS,** 36-item short-form survey physical component summary.

Supplemental digital content is available for this article at neurosurgery-online.com.

A major shortcoming in optimizing care for patients with cervical spondylotic myelopathy (CSM) is the lack of longitudinal imaging to track neurological recovery after surgery.[1] Spinal instrumentation introduces significant image artifact on postoperative films,[2,3] preventing clinicians and researchers from adequately assessing white matter tracts after decompression.

Few studies have investigated the ability of conventional MRI (ie, T1/T2 signal changes) to assess postoperative neurological status[4-6] and even fewer have examined postoperative diffusion-weighted imaging (DWI) techniques.[1,7-9] In addition, existing evidence is not only mixed but limited in clinical outcomes measured, focusing mainly on the modified Japanese Orthopedic Association (mJOA) score. Given this evidence gap, we evaluated the relationship between postoperative DWI measures, including diffusion tensor imaging (DTI) and the recently described diffusion basis spectrum imaging (DBSI),[10,11] and clinical markers of neurological recovery in patients with CSM at 2-year postoperative follow-up. Compared with traditional patient-reported outcome measures (PROMs), quantitative DBSI metrics detect objective changes in spinal cord microstructure and may have potential as biomarkers of spinal cord recovery to inform surgical prognosis and guide postoperative rehabilitation strategies.

METHODS

Study Design and Patient Population

A single center prospectively enrolled 50 patients with CSM from 2018 through 2020. Inclusion and exclusion criteria are defined in **Supplemental Digital Content 1, eTable 1** (http://links.lww.com/NEU/E317). All patients underwent anterior or posterior surgery based on surgeon discretion and were followed longitudinally for up to 2 years postoperatively. This study was approved by our institution's institutional review board and designed and reported per the strengthening the reporting of observational studies in epidemiology guidelines.[12] All patients completed informed consent.

Clinical Measures

PROMs were obtained preoperatively and postoperatively at 2-year follow-up. Neuromuscular function was evaluated by the mJOA[13] (minimal clinically important difference [MCID]: 2 points),[14] myelopathy disability index[15] (MDI; MCID: 2 points),[16] and disabilities of the arm, shoulder, and hand[17] (DASH; MCID: 10.8 points).[18] Patients were characterized as having mild (mJOA 15-17), moderate (mJOA 12-14), or severe (mJOA 0-11) myelopathy. Lower scores on the mJOA and higher scores on the MDI and DASH indicate worse functional status. Quality of life was assessed via the SF-36 physical (PCS) and mental (MCS) component summary scores (MCIDs: 4 points),[19] where higher values indicate better quality of life.[19] Neck pain–related disability was measured using the neck disability index (NDI, MCID: 7.5 points),[20] with higher scores denoting worse pain/disability.[21]

Imaging Technique

DWI was performed on a 3T Prisma (Siemens Healthcare) scanner with vendor-supplied sequences. All patients underwent DWI preoperatively and 2 years postoperatively. DTI modeling and DBSI modeling were performed on each patient in both the preoperative and postoperative time frames. DBSI models DWI signals from image voxels as a linear combination of anisotropic tensors, which describe axonal diffusion, and isotropic tensors, reflecting *extra*-axonal diffusion.[11] This is in contrast to DTI modeling, which assumes a single diffusion tensor averaging the diffusion profile of multiple microstructural compartments within an image voxel (Figure 1).[22]

A vendor-supplied ZOOMIt (Siemens Healthcare) sequence was used with the following parameters: acquisition time: ~2 min per scan; repetition time: 620 ms; echo time: 70 ms; in-plane resolution: 0.75 × 0.75 mm^2; four 7.5-mm-thick slices covering C3 to C6; cardiac gated; field of view: 76 × 38 cm^2; data matrix: 102 × 51. DWI data were obtained using a 26-direction diffusion weighting with maximum b-value = 1000 s/mm^2 (0-1000 at step of 40 distributed randomly assigned to each diffusion-weighting direction).

DBSI models DWI signals according to Eq. [1]:

$$S_k = \sum_{i=1}^{N_{Aniso}} f_i e^{-|\vec{b}_k|\lambda_{\perp i}} e^{-|\vec{b}_k|\left(\lambda_{\parallel i}-\lambda_{\perp i}\right)\cos^2\psi_{ik}} + \int_a^b f(D) e^{-|\vec{b}_k|} DdD \; (k=1,2,3,\ldots) \quad [1]$$

where S_k is the signal from the k^{th} diffusion gradient, $\vec{b}_k$ is the k^{th} b-value, f_i is the i^{th} signal intensity fraction, $\lambda_{\perp i}$ and $\lambda_{\parallel i}$ are the i^{th} axial and radial diffusivity, respectively, ψ_{ik} is the angle between the k^{th} gradient and the i^{th} fiber orientation, and D is the diffusivity coefficient determining an isotropic tensor.

A preprocessing pipeline developed in-house via Python (Python Software Foundation) was applied to diffusion-weighted images of the spinal cord to correct for motion artifact using a 2-dimensional registration protocol in the axial plane. For each spinal cord level, midsagittal T2-weighted images were used as an anatomic reference to extract axial slices of the spinal cord from diffusion-weighted images (Figure 2). Specifically, four 7.5-mm-thick slices from the C3 to C6 cervical spine levels (at the midvertebral level) were obtained. In this study, only DWI data from the C3 level were used. Hand-drawn regions of interest (ROIs) were manually applied on the white matter encompassing motor and sensory tracts. DTI/DBSI metrics were calculated for each voxel, per slice, per ROI using an in-laboratory Python-implemented pipeline. The median values of all voxels within the ROIs from each patient were grouped for statistical analysis.

Imaging Parameters

Supplemental Digital Content 1, eTable 2 (http://links.lww.com/NEU/E317) provides a summary of DTI/DBSI metrics. DTI-derived metrics included fractional anisotropy (FA), a reflection of overall white matter tract integrity,[23] apparent diffusion coefficient (ADC), axial diffusivity, and radial diffusivity. DBSI-derived anisotropic tensors included FA, fiber fraction, which reflects axonal density,[24] and axial and radial diffusivity. Decreasing axial diffusivity is thought to measure axonal injury, whereas increasing radial diffusivity represents demyelination.[24] DBSI-derived isotropic tensors use the ADC, which quantifies the magnitude of water diffusion,[11] to signify different pathologies. Isotropic tensors were classified to include restricted fraction (ADC ≤ 0.3 $\mu m^2/ms$), which quantifies cellularity,[25] and nonrestricted fraction (ADC > 0.3 $\mu m^2/ms$), a reflection of vasogenic edema and tissue loss.[26]

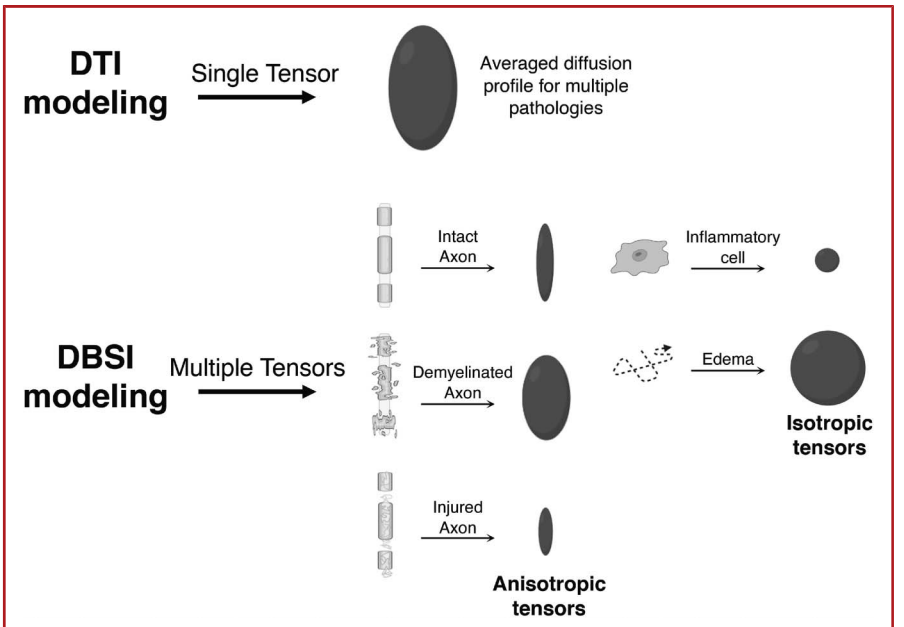

FIGURE 1. *DTI assumes a single tensor when interpreting the diffusion-weighted MRI signals within an image voxel. By contrast, DBSI models diffusion-weighted MRI signals as a linear combination of anisotropic tensors, reflecting directionally dependent diffusion of water, and isotropic tensors, which describes the uniform diffusion of water. DBSI, diffusion basis spectrum imaging; DTI, diffusion tensor imaging. Reproduced from Zhang JK, Jayasekera D, Javeed S, Greenberg JK, et al. Diffusion basis spectrum imaging predicts long-term clinical outcomes following surgery in cervical spondylotic myelopathy. Spine J. 2023;23(4):504-512, with permission.*

Statistical Analyses

Descriptive data were analyzed using univariate statistics. Normality was evaluated via Shapiro–Wilk tests and linearity of relationships was visually assessed. Spearman's correlation (r_s) was performed to compare DTI/DBSI metrics with clinical variables, including the mJOA and PROMs. In accordance with Evans's classifications,[27] Spearman's correlation coefficients (r_s) <0.20 were considered "very weak," 0.20 to 0.39 "weak," 0.40 to 0.59 "moderate," 0.60 to 0.79 "strong," and ≥0.80 "very strong." *P*-values <.05 were determined a priori to be statistically significant. Because of our small sample size and the exploratory nature of our analysis, multiple comparisons testing was not performed. All statistical analyses were performed in R (Version 4.1.2).

RESULTS

Among the 50 patients who were initially included, 3 were excluded for clinical reasons (**Supplemental Digital Content 1, eFigure 1 and eTable 3**, http://links.lww.com/NEU/E317). One patient underwent preoperative evaluation but ultimately did not undergo surgery and 2 were found at later visits to have conditions that violated the inclusion criteria (severe lumbar stenosis and multiple comorbidities). Among the remaining 47 patients, 5 patients were excluded for poor MRI data quality. Of these, 4 patients were excluded because of significant motion artifact and 1 patient was confounded by a loop recorder. At 2-year follow-up, 9 (18%) patients with CSM were lost to follow-up, which was just under the 20% loss-to-follow-up threshold that is generally considered to introduce serious threats to study validity.[28] Three patients canceled appointments and did not reschedule because of the ongoing COVID-19 pandemic (2020-2022).[29] Three patients were unable to undergo repeat MRI because of medical concerns (ie, Tourette's syndrome, newly implanted non–MRI-compatible device, and O_2 requirements), 2 patients were unresponsive, and 1 patient had moved to a different state. Of the 33 remaining patients, 6 failed postoperative MRI processing. Specifically, 5 patients possessed significant instrumentation artifact and 1 patient had significant motion artifact (ie, patient movement during the scan) that precluded adequate analysis. As such, 22% (11/50) of patients were excluded because of MRI processing issues and 24% (12/50) were excluded for clinical or study logistical reasons. Ultimately, 27 patients, including 15 (56%) patients with mild CSM, 7 (26%) patients with moderate CSM, and 5 (19%) patients with severe CSM with a mean follow-up of 23.5 (SD 4.1, range 11-31) months, possessed complete clinical and DWI data for analysis.

Most patients were male (67%), with an average age of 56.7 ± 7.7 years and an average symptom duration of 33.3 ± 60 months

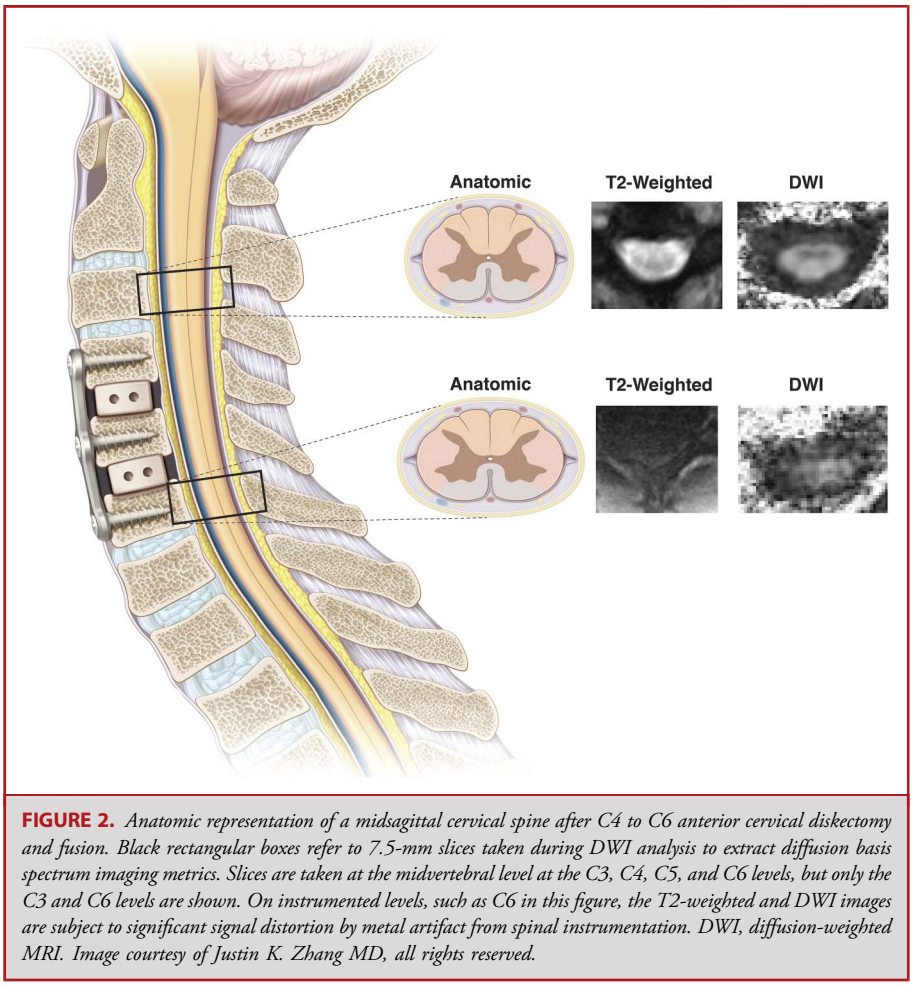

FIGURE 2. *Anatomic representation of a midsagittal cervical spine after C4 to C6 anterior cervical diskectomy and fusion. Black rectangular boxes refer to 7.5-mm slices taken during DWI analysis to extract diffusion basis spectrum imaging metrics. Slices are taken at the midvertebral level at the C3, C4, C5, and C6 levels, but only the C3 and C6 levels are shown. On instrumented levels, such as C6 in this figure, the T2-weighted and DWI images are subject to significant signal distortion by metal artifact from spinal instrumentation. DWI, diffusion-weighted MRI. Image courtesy of Justin K. Zhang MD, all rights reserved.*

(Table 1). Our study demographic sample, which was mostly White race (78%), roughly reflected the racial makeup of our patient population, which is 79.9% White. The median number of Elixhauser comorbidities was 1 (range 0-6), and approximately half (48%) of the cohort were tobacco users at the time of surgery. Most surgeries were multilevel (89%), with 17 (63%) patients receiving anterior and 10 (37%) patients receiving posterior surgery. Of our 27 included patients, there were 69 stenosed levels, which were defined on neuroradiology impressions as grade of spinal canal stenosis[30] greater than or equal to Grade 1 (**Supplemental Digital Content 1, eTable 4**, http://links.lww.com/NEU/E317). Among these stenosed segments, 52 levels were decompressed based on clinical presentation and severity of imaging pathology. Five of 27 (19%) patients were instrumented at the C3 level. Approximately half of the patients reached the MCID of the reported PROMs: mJOA (n = 10, 37%), SF-36 PCS (n = 17, 63%), SF-36 MCS (n = 13, 48%), NDI (n = 13, 48%), MDI (n = 11, 41%), and DASH (n = 15, 56%) (Table 2).

Imaging Parameters

Postoperative C3 slice DWI data were analyzed and correlated with postoperative clinical outcomes at 2-year follow-up. Correlation matrices depicting both DTI/DBSI metrics are displayed in Figure 3. Specifically, these tests were cross-sectional, postoperative DTI/DBSI and clinical outcome values at 2-year follow-up, not *change* in these metrics. Only significant correlations are shown. Complete correlation analyses comparing postoperative DWI-derived metrics with postoperative clinical assessments are documented in **Supplemental Digital Content 1, eTable 5** (http://links.lww.com/NEU/E317).

Twenty-four correlation tests were run comparing postoperative DTI metrics and postoperative CSM clinical measures. Of these, only DTI ADC (r_s = 0.35, P = .02), DTI FA (r_s = −0.35, P = .02), and DTI radial diffusivity (r_s = 0.37, P = .01) were weakly correlated with NDI (Figure 3). By contrast, of 36 correlations analyzed among postoperative DBSI metrics, there were

TABLE 1. Baseline Characteristics of CSM Cohort (N = 27)

Characteristics	Value
Age, y	56.7 (7.7)
BMI, kg/m^2	29 (6.2)
Sex, M:F	18:9 (67/33%)
Tobacco use	13 (48%)
Elixhauser comorbidities, no.	1 (0-6)
Symptom duration, mo	33.3 (60)
Left hand dynamometry, kW	65.3 (26.9)
Right hand dynamometry, kW	65.7 (24.9)
Positive Babinski reflex, no.	4 (15%)
Positive Hoffmann reflex, no.	15 (56%)
mJOA classification	
Mild	15 (56%)
Moderate	7 (26%)
Severe	5 (19%)
Surgery type	
ACDF	17 (63%)
Laminoplasty	10 (37%)
No. of levels	
Single	3 (11%)
Multilevel	24 (89%)
Follow-up, mo	23.5 (4.1)

ACDF, anterior cervical discectomy and fusion; BMI, body mass index; CSM, cervical spondylotic myelopathy; mJOA, modified Japanese Orthopedic Association.

10 significant correlations. The highest-magnitude relationships were a strong positive correlation between DBSI axial diffusivity and the NDI (r_s = 0.60, P < .001), a moderate negative association between DBSI fiber fraction and the NDI (r_s = −0.58, P < .001), and a moderate positive correlation between DBSI restricted fraction and the NDI (r_s = 0.56, P<.001). The weakest correlation was between DBSI radial diffusivity and the SF-36 PCS (r_s = −0.45, P = .02). DBSI axial diffusivity and DBSI fiber fraction were both correlated with 3 clinical outcome measures: NDI, MDI, and DASH. Of all postoperative clinical measures, the NDI possessed the most significant correlations with both DTI- and DBSI-derived metrics (7/13 significant correlations, 54%). In comparison, the mJOA and SF-36 MCS were not significantly correlated with any DWI-derived measures.

DISCUSSION

Postoperative DWI in CSM

Our results demonstrate that postoperative DWI is not only feasible but can effectively characterize neuromuscular function, quality of life, and pain at 2-year follow-up after surgery. Overall, the relationship between imaging and clinical variables was expected, in that worsening DWI metrics were associated with worse clinical outcomes. For example, DBSI fiber fraction was *negatively* correlated with the NDI, demonstrating that lower axonal density was associated with greater pain-related disability. DBSI radial diffusivity was *negatively* correlated with the SF-36 PCS, suggesting that increasing markers of demyelination were related to worse general physical health. However, DBSI restricted fraction and nonrestricted fraction were *positively* correlated with the NDI, indicating that increased cellularity/inflammation and vasogenic edema were both associated with greater pain-related disability. Similar correlations were appreciated between DTI metrics and clinical outcomes but to a lesser degree. Specifically, DBSI metrics possessed a higher proportion of significant correlations (10/36 total tests, 28%) with higher magnitude (range r_s: 0.39-0.60) than DTI parameters (3/24 total tests, 13%) (range r_s: 0.34-0.37). These results suggest that DBSI metrics may serve as more sensitive and specific biomarkers of surgical recovery than DTI parameters.

In addition, evaluations of quality of life capture important but different aspects of the postoperative course and therefore should be measured in tandem with functional outcomes.[31,32] Although there were significant correlations between DBSI and SF-36 PCS measures, we did not find significant associations for the SF-36 MCS. Although psychological distress is a known component of CSM,[33] this was an expected result, as we did not expect quantitative measurements of spinal cord microstructure to correlate with mental health.

Findings in Context

Our results support existing literature by demonstrating that surgical decompression for CSM is associated with significant improvements across comprehensive clinical outcomes.[13] Given that CSM pathophysiology is characterized by chronic neural tissue degeneration,[34] the ability of DWI metrics to objectively measure spinal cord integrity after decompression may serve as an important adjunct to established clinical domains. For example, Fehlings et al[35] recently investigated the neuroprotective role of riluzole in enhancing neurological recovery after decompression for patients with CSM. Although riluzole was not associated with superior improvements in mJOA, there may have been differences in spinal cord microstructure detectable using DBSI, a potential phenomenon that can be investigated in future work.

Our group has previously investigated the utility of preoperative MRI in assessing baseline disease severity[36,37] and prognosticating long-term clinical outcomes. As a supplemental analysis in this paper, we also found that, to a lesser extent,

TABLE 2. Baseline and Change in Clinical Outcome Measures

	Outcome measure					
Variable	**mJOA**	**SF-36 PCS**	**SF-36 MCS**	**NDI**	**MDI**	**DASH**
Preoperative	14.3 (3)	37.7 (10.2)	45.1 (13.6)	19.2 (11.7)	5.3 (6)	35 (25.4)
Postoperative	15.6 (2.6)	43.6 (12.2)	49 (12.9)	12.1 (12.7)	3.8 (5.3)	22.9 (26.2)
Change	**1.3 (1.9)**[a]	**5.9 (8.4)**[a]	3.9 (9.8)	**−7.1 (5.4)**[a]	**−1.5 (2.5)**[a]	**−12.2 (11.3)**[a]
Achieved MCID (%)[b]	10 (37%)	17 (63%)	13 (48%)	13 (48%)	11 (41%)	15 (56%)

DASH, disability of the arm shoulder and hand; MCID, minimal clinically important difference; MDI, myelopathy disability index; mJOA, modified Japanese Orthopedic Association; NDI, neck disability index; SF-36 MCS, 36-item short-form survey mental component summary; SF-36 PCS, 36-item short-form survey physical component summary.
[a]Bold values indicate statistical significance ($P < .005$) on pairwise *t*-tests.
[b]MCIDs for each clinical outcome were as follows: mJOA (2 points); SF-36 PCS (4 points); SF-36 MCS (4 points); NDI (7.5 points); MDI (3 points); DASH (10.8 points).

preoperative DWI metrics were significantly correlated with postoperative clinical outcomes at 2-year follow-up, including both cross-sectional and change (Δ) values (**Supplemental Digital Content 1, eTable 6**, http://links.lww.com/NEU/E317). A similar trend was appreciated with respect to the pattern of significance, in that only one DTI variable was significantly associated with postoperative outcomes (DTI radial diffusivity vs ΔmJOA r = −0.317, $P = .04$) compared with 10 significant correlations with DBSI metrics, the strongest association between DBSI restricted fraction and postoperative PCS (r = −0.41, r = 0.008). The latter result is consistent with previously described notions that the extra-axonal component of CSM pathology may play a significant role in disease severity and possibly longer-term outcomes.[16] The results of this study complement the previous findings that assess the utility of *preoperative* DWI metrics. Specifically, they suggest that DWI is not only feasible in the

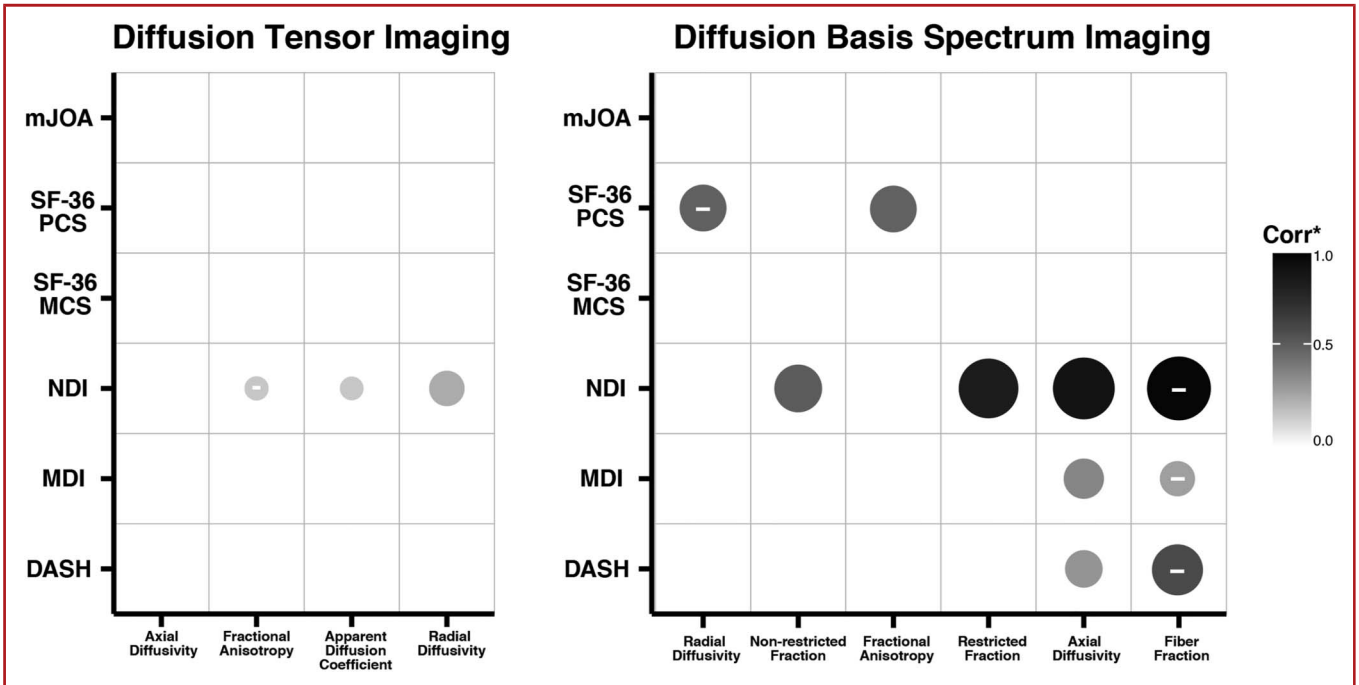

FIGURE 3. *Correlation matrices of diffusion tensor imaging and diffusion basis spectrum imaging parameters (x-axis) with cervical spondylotic myelopathy clinical measures (y-axis). Only significant correlations ($P < .05$) are shown. Larger and darker circles represent greater magnitude of the correlation. *All correlations are positive unless indicated with (−) sign. DASH, disability of the arm shoulder and hand; MDI, myelopathy disability index; mJOA, modified Japanese Orthopedic Association; NDI, neck disability index; SF-36 MCS, 36-item short-form survey mental component summary; SF-36 PCS, 36-item short-form survey physical component summary.*

postoperative setting and correlates with postoperative outcomes, but may potentially serve as a useful adjunct to assess spinal cord integrity after decompression.[10,16]

To that end, we emphasize that the purpose of this study is *not* to suggest that DWI in its current form can *predict* postoperative recovery or long-term clinical outcomes. Research on the utility of postoperative imaging modalities in CSM may provide meaningful insights on optimal postoperative rehabilitation strategies. For example, postoperative DBSI may have the potential to identify poor responders to surgical intervention before significant clinical symptoms arise, providing an opportunity to pursue aggressive nonoperative therapy or close monitoring with serial follow-up examinations.

Limitations

An inherent limitation of this study is that the evaluation of the spinal cord was exclusively at the mostly noninstrumented C3 level. However, this approach has been implemented in previous studies[7] and was similarly performed in our study for 2 reasons. First, the majority of surgeries in our cohort involved instrumentation at the C4 to C6 vertebral levels, and DWI data from these spinal levels produced significant image artifacts on analysis.[3,38-40] Second, imaging additional cervical spinal levels (ie, C1, C2, and C7) not only increased scanner time, augmenting costs, and patient burden, but produced DWI data more difficult to model because of partial volume effects.[41,42]

For these reasons, we elected to focus on the rostral C3, mostly noninstrumented level. This approach allowed us to not only extract more accurate spinal cord data but also maintain homogeneous patient data. One critique of this approach is that the majority of stenotic levels did not include C3, and therefore, functional prognosis based on this ROI that may not be the main driver of clinical symptoms is less useful. However, there is a growing body of literature that has demonstrated microstructural changes in the spinal cord remote from the core lesion. Specifically, recent basic and translation science research has reported retrograde axonal degeneration and cranial spread of disease in the setting of spinal cord injury.[34,43]

In our study, 11 patients failed MRI processing (5 preoperatively and 6 postoperatively). Broadly speaking, preoperative MRI processing failed because of motion artifact, whereas postoperative MRI processing failed because of instrumentation artifact. Motion artifact is a broad term that refers to physical motion from the patient moving as well as internal cardiac and respiratory physiologic artifact. It is important to note, however, that there are a handful of other reasons that contribute to poor signal acquisition during MRI, including obesity (ie, fat contaminant), severe spinal cord compression (making it difficult to differentiate white and gray matter for ROI mapping), anatomy (eg, severe cervical lordosis), and postoperative edema.[44] Even under perfect conditions, attaining high-resolution spinal cord images is difficult because of bony anatomy surrounding the spinal canal, physiological motion, and small cross-sectional dimensions.[45] DWI is even more reliant on high-quality images, and therefore, additional artifact (ie, motion and metallic) can often significantly confound analysis.

Because the utility of postoperative MRI has been poorly characterized and rarely investigated in the CSM literature, largely because of technical limitations, one of the main purposes of our study is to serve as a methodological proof of concept. Specifically, we emphasize that postoperative DWI is difficult but feasible when judiciously selecting viable spinal segments and meticulously drawing reliable ROIs. Although a large number of patients were excluded because of methodological constraints (ie, 22% (11/50) of MRI processing failure), this is not entirely unexpected. Current efforts are underway in our methods development to better control for both motion and instrumentation artifacts to increase the clinical feasibility of diffusion MRI for spinal cord pathologies.

Along similar lines, because this study was exploratory in nature, multiple comparisons tests were not performed, increasing our risk for Type 1 errors. Indeed, when applying a false discovery rate correction for multiple comparisons, the number of significant correlations decreased from 13 (out of 72 total tests) to 4. Although these shortcomings limit the interpretability of our results, they nonetheless provide a basis for the feasibility and applicability of postoperative MRI in CSM. Moving forward, we are actively planning to validate our results in larger sample sizes across different patient populations and imaging platforms at other institutions.

CONCLUSION

Objective measurements of spinal cord integrity derived from DWI may have utility as biomarkers of surgical recovery for patients with CSM after decompressive surgery. Postoperative DBSI metrics showed multiple significant correlations with neuromuscular function, quality of life, and pain outcomes at long-term follow-up. These quantifiable metrics of spinal cord microstructure may enhance prediction of recovery trajectories for patients with CSM after surgery.

Funding

This work was supported by the National Institute of Neurological Disorders and Stroke, Grant Numbers: R01 - NS047592 (Wilson Z. Ray/Sheng-Kwei Song); U01- EY025500 (Sheng-Kwei Song). This work was also supported by the National Center for Advancing Translational Sciences of the National Institutes of Health under Award Number TL1TR002344 (Justin K. Zhang). The content of this article is solely the responsibility of the authors and does not necessarily represent the official views of the funding agency.

Disclosures

Andrew T. Dailey receives funding from Zimmer Biomet and AO North America. Erica F. Bisson is a consultant for Stryker, MiRus, and Medtronic, and has equity interest in NView Medical, Proprio, and

SeeALL. Marcus Mazur is a consultant for Medtronic, reports fellowship support and personal fees from Cerapedics outside the submitted work, and has a patent for motorized skeletal traction, patent No. 18/114,157. The other authors have no personal, financial, or institutional interest in any of the drugs, materials, or devices described in this article.

REFERENCES

1. Rajasekaran S, Kanna RM, Chittode VS, Maheswaran A, Aiyer SN, Shetty AP. Efficacy of diffusion tensor imaging indices in assessing postoperative neural recovery in cervical spondylotic myelopathy. *Spine.* 2017;42(1):8-13.
2. Ahmad FU, Sidani C, Fourzali R, Wang MY. Postoperative magnetic resonance imaging artifact with cobalt-chromium versus titanium spinal instrumentation: presented at the 2013 Joint Spine Section Meeting. *J Neurosurg Spine.* 2013;19(5):629-636.
3. Leclet H. Artifacts in magnetic resonance imaging of the spine after surgery with or without implant. *Eur Spine J.* 1994;3(5):240-245.
4. Arvin B, Kalsi-Ryan S, Karpova A, et al. Postoperative magnetic resonance imaging can predict neurological recovery after surgery for cervical spondylotic myelopathy: a prospective study with blinded assessments. *Neurosurgery.* 2011;69(2):362-368.
5. Kato S, Nouri A, Reihani-Kermani H, Oshima Y, Cheng J, Fehlings MG. Postoperative resolution of magnetic resonance imaging signal intensity changes and the associated impact on outcomes in degenerative cervical myelopathy: analysis of a global cohort of patients. *Spine.* 2018;43(12):824-831.
6. Machino M, Ando K, Kobayashi K, et al. Postoperative changes in spinal cord signal intensity in patients with spinal cord injury without major bone injury: comparison between preoperative and postoperative magnetic resonance images. *J Neurosurg Spine.* 2020;34(2):259-266.
7. Ma X, Han X, Jiang W, et al. A follow-up study of postoperative DCM patients using diffusion MRI with DTI and NODDI. *Spine (Phila Pa 1976).* 2018;43(15):e898-e904.
8. Kitamura M, Maki S, Koda M, et al. Longitudinal diffusion tensor imaging of patients with degenerative cervical myelopathy following decompression surgery. *J Clin Neurosci.* 2020;74:194-198.
9. Zhang H, Guan L, Hai Y, Liu Y, Ding H, Chen X. Multi-shot echo-planar diffusion tensor imaging in cervical spondylotic myelopathy. *Bone Joint J.* 2020;102-b(9):1210-1218.
10. Jayasekera D, Zhang JK, Blum J, et al. Analysis of combined clinical and diffusion basis spectrum imaging metrics to predict the outcome of chronic cervical spondylotic myelopathy following cervical decompression surgery. *J Neurosurg Spine.* 2022;37(4):588-598.
11. Cross AH, Song S-K. A new imaging modality to non-invasively assess multiple sclerosis pathology. *J Neuroimmunol.* 2017;304:81-85.
12. von Elm E, Altman DG, Egger M, et al. The Strengthening the Reporting of Observational Studies in Epidemiology (STROBE) statement: guidelines for reporting observational studies. *J Clin Epidemiol.* 2008;61(4):344-349.
13. Badhiwala JH, Ahuja CS, Akbar MA, et al. Degenerative cervical myelopathy—update and future directions. *Nat Rev Neurol.* 2020;16(2):108-124.
14. Tetreault L, Nouri A, Kopjar B, Côté P, Fehlings MG. The minimum clinically important difference of the Modified Japanese Orthopaedic Association scale in patients with degenerative cervical myelopathy. *Spine (Phila Pa 1976).* 2015;40(21):1653-1659.
15. Casey AT, Bland JM, Crockard HA. Development of a functional scoring system for rheumatoid arthritis patients with cervical myelopathy. *Ann Rheum Dis.* 1996;55(12):901-906.
16. Zhang JK, Jayasekera D, Javeed S, et al. Diffusion basis spectrum imaging predicts long-term clinical outcomes following surgery in cervical spondylotic myelopathy. *Spine J.* 2023;23(4):504-512.
17. Hudak PL, Amadio PC, Bombardier C. Development of an upper extremity outcome measure: the DASH (disabilities of the arm, shoulder and hand) [corrected]. The Upper Extremity Collaborative Group (UECG). *Am J Ind Med.* 1996;29(6):602-608.
18. Franchignoni F, Vercelli S, Giordano A, Sartorio F, Bravini E, Ferriero G. Minimal clinically important difference of the disabilities of the arm, shoulder and hand outcome measure (DASH) and its shortened version (QuickDASH). *J Orthop Sports Phys Ther.* 2014;44(1):30-39.
19. Badhiwala JH, Witiw CD, Nassiri F, et al. Minimum clinically important difference in SF-36 scores for use in degenerative cervical myelopathy. *Spine (Phila Pa 1976).* 2018;43(21):e1260-e1266.
20. Carreon LY, Glassman SD, Campbell MJ, Anderson PA. Neck Disability Index, short form-36 physical component summary, and pain scales for neck and arm pain: the minimum clinically important difference and substantial clinical benefit after cervical spine fusion. *Spine J.* 2010;10(6):469-474.
21. Kalsi-Ryan S, Singh A, Massicotte EM, et al. Ancillary outcome measures for assessment of individuals with cervical spondylotic myelopathy. *Spine (Phila Pa 1976).* 2013;38(22 Suppl 1):S111-S122.
22. Le Bihan D, Mangin J-F, Poupon C, et al. Diffusion tensor imaging: concepts and applications. *J Magn Reson Imaging JMRI.* 2001;13(4):534-546.
23. Shabani S, Kaushal M, Budde MD, Wang MC, Kurpad SN. Diffusion tensor imaging in cervical spondylotic myelopathy: a review. *J Neurosurg Spine.* 2020;33(1):65-72.
24. Song SK, Sun SW, Ju WK, Lin SJ, Cross AH, Neufeld AH. Diffusion tensor imaging detects and differentiates axon and myelin degeneration in mouse optic nerve after retinal ischemia. *Neuroimage.* 2003;20(3):1714-1722.
25. Wang Y, Wang Q, Haldar JP, et al. Quantification of increased cellularity during inflammatory demyelination. *Brain.* 2011;134(Pt 12):3590-3601.
26. Chiang CW, Wang Y, Sun P, et al. Quantifying white matter tract diffusion parameters in the presence of increased extra-fiber cellularity and vasogenic edema. *Neuroimage.* 2014;101:310-319.
27. Evans JD. *Straightforward Statistics for the Behavioral Sciences*. Thomson Brooks/Cole Publishing Co; 1996.
28. Dettori JR. Loss to follow-up. *Evid Based Spine Care J.* 2011;2(1):7-10.
29. Subathra GN, Rajendrababu SR, Senthilkumar VA, Mani I, Udayakumar B. Impact of COVID-19 on follow-up and medication adherence in patients with glaucoma in a tertiary eye care centre in south India. *Indian J Ophthalmol.* 2021;69(5):1264-1270.
30. Kang Y, Lee JW, Koh YH, et al. New MRI grading system for the cervical canal stenosis. *AJR Am J Roentgenol.* 2011;197(1):W134-W140.
31. Spurgas MP, Abbas SF, Szewczyk BS, Yim B, Ata A, German JW. The effect of length of follow-up on substantial clinical benefit thresholds in patients undergoing surgery for cervical degenerative myelopathy. *J Clin Neurosci.* 2019;62:88-93.
32. Lubelski D, Alvin MD, Nesterenko S, et al. Correlation of quality of life and functional outcome measures for cervical spondylotic myelopathy. *J Neurosurg Spine.* 2016;24(3):483-489.
33. Young SB, Aprill C, Braswell J, Ogard WK, Richards JS, McCarthy JP. Psychological factors and domains of neck pain disability. *Pain Med.* 2009;10(2):310-318.
34. Akter F, Kotter M. Pathobiology of degenerative cervical myelopathy. *Neurosurg Clin N Am.* 2018;29(1):13-19.
35. Fehlings MG, Badhiwala JH, Ahn H, et al. Safety and efficacy of riluzole in patients undergoing decompressive surgery for degenerative cervical myelopathy (CSM-Protect): a multicentre, double-blind, placebo-controlled, randomised, phase 3 trial. *Lancet Neurol.* 2021;20(2):98-106.
36. Zhang JK, Jayasekera D, Song C, et al. Diffusion basis spectrum imaging provides insights into cervical spondylotic myelopathy pathology. *Neurosurgery.* 2023;92(1):102-109.
37. Zhang JK, Sun P, Jayasekera D, et al. Utility of diffusion basis spectrum imaging in quantifying baseline disease severity and prognosis of cervical spondylotic myelopathy. *Spine.* 2022;47(24):1687-1693.
38. Ernstberger T, Heidrich G, Schultz W, Grabbe E. Implant detectibility of intervertebral disc spacers in post fusion MRI: evaluation of the MRI scan quality by using a scoring system—an in vitro study. *Neuroradiology.* 2007;49(2):103-109.
39. Rudisch A, Kremser C, Peer S, Kathrein A, Judmaier W, Daniaux H. Metallic artifacts in magnetic resonance imaging of patients with spinal fusion. A comparison of implant materials and imaging sequences. *Spine (Phila Pa 1976).* 1998;23(6):692-699.
40. Yang C-W, Liu L, Wang J, et al. Magnetic resonance imaging of artificial lumbar disks: safety and metal artifacts. *Chin Med J.* 2009;122(8):911-916.
41. González Ballester MA, Zisserman AP, Brady M. Estimation of the partial volume effect in MRI. *Med Image Anal.* 2002;6(4):389-405.
42. Salminen LE, Conturo TE, Bolzenius JD, Cabeen RP, Akbudak E, Paul RH. Reducing CSF partial volume effects to enhance diffusion tensor imaging metrics of brain microstructure. *Technol Innov.* 2016;18(1):5-20.
43. David G, Mohammadi S, Martin AR, et al. Traumatic and nontraumatic spinal cord injury: pathological insights from neuroimaging. *Nat Rev Neurol.* 2019;15(12):718-731.
44. Krupa K, Bekiesińska-Figatowska M. Artifacts in magnetic resonance imaging. *Pol J Radiol.* 2015;80:93-106.
45. Stroman PW, Wheeler-Kingshott C, Bacon M, et al. The current state-of-the-art of spinal cord imaging: methods. *Neuroimage.* 2014;84:1070-1081.

Acknowledgments

Author Contributions: Justin K. Zhang MD MSCI: Formal analysis; Investigation; Methodology; Project administration; Visualization; Roles/Writing—original draft; Validation; Writing—review and editing; Saad Javeed MD, MSCI: Formal analysis; Methodology; Project administration; Visualization; Roles/Writing—original draft; Validation; Writing—review and editing; Jacob K. Greenberg MD MSCI: Formal analysis; Methodology; Project administration; Visualization; Roles/Writing—original draft; Validation; Writing—review and editing; Salim Yakdan MD MSCI: Formal analysis; Methodology; Project administration; Visualization; Roles/Writing—original draft; Validation; Writing—review and editing; Muhammad I. Kaleem MBBS: Formal analysis; Methodology; Project administration; Visualization; Roles/Writing—original draft; Validation; Writing—review and editing; Kathleen S. Botterbush BS: Formal analysis; Methodology; Project administration; Visualization; Roles/Writing—original draft; Validation; Writing—review and editing; Braeden Benedict BS: Formal analysis; Methodology; Project administration; Visualization; Roles/Writing—original draft; Validation; Writing—review and editing; Christopher F. Dibble MD PhD: Investigation; Methodology; Project administration; Supervision; Validation; Writing—review and editing; Peng Sun PhD: Investigation; Methodology; Project administration; Supervision; Validation; Writing—review and editing; Brandon Sherrod MD: Investigation; Methodology; Project administration; Supervision; Validation; Writing—review and editing; Andrew T. Dailey MD: Investigation; Methodology; Project administration; Supervision; Validation; Writing—review and editing; Erica F. Bisson MD MPH: Investigation; Methodology; Project administration; Supervision; Validation; Writing—review and editing; Mark Mahan MD: Investigation; Methodology; Project administration; Supervision; Validation; Writing—review and editing; Marcus Mazur MD: Investigation; Methodology; Project administration; Supervision; Validation; Writing—review and editing. Sheng-Kwei Song PhD: Investigation; Methodology; Project administration; Supervision; Validation; Writing—review and editing; Wilson Z. Ray MD: Investigation; Methodology; Project administration; Supervision; Validation; Writing—review and editing.

Supplemental digital content *is available for this article at neurosurgery-online.com.*

Supplemental Digital Content 1. eFigure 1. A flowchart showing the patients recruited and ultimately included in the study analyses. **eTable 1.** Inclusion and exclusion criteria. **eTable 2.** Diffusion-weighted MRI (DWI) parameters. **eTable 3.** Reasons for participant exclusion from final analysis. **eTable 4.** Grade of spinal canal stenosis as defined by Kang et al. **eTable 5.** Spearman correlations between clinical outcomes and DWI parameters. **eTable 6.** Correlation between preoperative DWI metrics (DTI and DBSI) and postoperative patient-reported outcome measures (PROMs).